

Tunable circularly polarized lasing emission in reflection distributed feedback dye lasers

Fei Chen,¹ Denis Gindre,¹ and Jean-Michel Nunzi^{2,*}

¹Laboratoire POMA, FRE CNRS 2988, Université d'Angers, 2 Boulevard Lavoisier, 49045 Angers, France

²Department of Physics and Chemistry, Queen's University, Kingston K7L 3N6, Ontario, Canada

*Corresponding author: nunzjm@queensu.ca

Abstract: A tunable circularly polarized distributed feedback (DFB) laser based on reflection grating configuration was realized in a solution of 4-(dicyanomethylene)-2-methyl-6-(4-dimethylaminostyryl)-4H-pyran (DCM) doped methanol. Chiral photonic DFB structures with tunable photonic bandgap were generated by controlling the state of polarization of the two interfering pump beams. The dual-peak lasing emission spectrum indicates that the periodic chiral DFB grating is affected by a combination of modulations of gain and refractive index.

©2008 Optical Society of America

OCIS codes: (140.3490) Distributed-feedback; (120.5700) Reflection; (260.5430) Polarization; (140.2050) Dye lasers recording materials.

References and links:

1. H. Kogelnik and C. V. Shank, "Simulated emission in a periodic structure," *Appl. Phys. Lett.* **18**, 152-154 (1971).
2. D. Gindre, A. Vesperini, J.-M. Nunzi, H. Leblond and K. D. Dorkenoo, "Refractive-index saturation-mediated multiple line emission in polymer thin-film distributed feedback lasers," *Opt. Lett.* **31**, 1657-1659 (2006).
3. J. Wang, C. Ye, F. Chen, L. Shi and D. Lo, "Wavelength tunable two-photon-pumped distributed feedback zirconia waveguide lasers," *J. Opt. A: Pure Appl. Opt.* **7**, 261-264 (2005).
4. F. Chen, J. Wang, C. Ye, W. H. Ni, J. Chan, Y. Yang and D. Lo, "Near infrared distributed feedback lasers based on LDS dye-doped zirconia organically modified silicate channel waveguides," *Opt. Express* **13**, 1643-1650 (2005).
5. Y. J. Liu, X. W. Sun, P. Shum, H. P. Li, J. Mi, W. Ji and X. H. Zhang, "Low-threshold and narrow-linewidth lasing from dye-doped holographic polymer-dispersed liquid crystal transmission gratings," *Appl. Phys. Lett.* **88**, 061107 (2006).
6. D. E. Lucchetta, L. Criante, O. Francescangeli and F. Simoni, "Light amplification by dye-doped holographic polymer dispersed liquid crystals," *Appl. Phys. Lett.* **84**, 4893-4895 (2004).
7. S.-T. Wu and A. Y.-G. Fuh, "Lasing in photonic crystal based on dye-doped holographic polymer-dispersed liquid crystal reflection gratings," *Conference Lasers and Electro-Optics CLEO*, **3**, 2218-2220 (2005)
8. F. Chen, D. Gindre and J.-M. Nunzi, "First-order distributed feedback dye laser effect in reflection pumping geometry," *Opt. Lett.* **32**, 805-807 (2007).
9. D. Lo, C. Ye, and J. Wang, "Distributed feedback laser action by polarization modulation," *Appl. Phys. B* **76**, 649-653 (2003).
10. C. Ye, J. Wang, L. Shi and D. Lo, "Polarization and threshold energy variation of distributed feedback lasing of oxazine dye in zirconia waveguides and in solutions," *Appl. Phys. B* **78**, 189 (2004).
11. V. I. Kopp, Z. Q. Zhang and A. Z. Genack, "Lasing in chiral photonic structures," *Quantum. Electron.* **27**, 369-416 (2003).
12. E. Yablonovitch, "Inhibited spontaneous emission in solid-state physics and electronics," *Phys. Rev. Lett.* **58**, 2059-2062 (1987).
13. V. I. Kopp, B. Fan, H. K. M. Vithana and A. Z. Genack, "Low-threshold lasing at a edge of a photonic stop band in cholesteric liquid crystals," *Opt. Lett.* **23**, 1707-1709 (1998).
14. Y. Matsuhisa, Y. H. Huang, Y. Zhou, S.-T. Wu, R. Ozaki, Y. Takao, A. Fujii and M. Ozaki, "Low-threshold and high efficiency lasing upon band-edge excitation in a cholesteric liquid crystal," *Appl. Phys. Lett.* **90**, 091114 (2007).
15. H. Kogelnik and C. V. Shank, "Coupled-wave theory of distributed feedback lasers," *J. Appl. Phys.* **43**, 2327-2335 (1972).
16. T. Z. Huang and K. H. Wagner, "Coupled Mode Analysis of Polarization Volume Hologram," *IEEE J. Quantum Electron.* **31**, 372-390 (1995).

1. Introduction

The distributed feedback (DFB) technique has been intensively employed for achieving tunable lasers since the first DFB laser was pioneered by Kogelnik and Shank [1]. Gindre *et al.* obtained refractive-index saturation-mediated multiple line emission with a Lloyd mirror device [2]. Lo's group realized dynamic DFB waveguide lasers using two crossing pump beams [3, 4]. Low-threshold and narrow-linewidth lasing was observed in a photonic bandgap (PBG) structure composed of a dye doped holographic polymer-dispersed liquid crystal (H-PDLC) by using holography technique [5]. All the above-mentioned DFB lasers were operated in a traditional transmission grating geometry. Recently, light amplification and a DFB lasing were obtained in a photonic crystal (PC) based on dye doped H-PDLC by Lucchetta *et al.* and Wu *et al.* respectively [6, 7]. In their work, instead of the traditional transmission DFB grating geometry, a DFB lasing was achieved in a reflection grating geometry constructed by two interfering pump beams coming from the opposite sides of the sample. In this case, the grating vector was perpendicular to the surface of the sample. In our latest work, a dynamic dual-peak DFB lasing action was successfully demonstrated in a reflection pumping geometry [8]. In early work, a DFB lasing feedback was provided by periodic spatial modulations of either gain or index or a combination of both in the gain medium. For the dynamic DFB lasers with two interfering beams, the intensity modulation, caused by a light intensity pattern induced gain and/or refractive index DFB gratings. Notably, polarization modulation was also introduced into DFB lasers for the optical feedback. Lo's group reported a detailed experimental investigation of the polarization properties of a DFB lasing output by polarization modulation based on dye doped solutions and dye doped sol-gel waveguides in the conventional transmission pumping geometry [9, 10]. They demonstrated that a transient polarization grating induced by the optical anisotropy of the gain medium resulting from polarization modulation can be used to generate DFB laser action.

It is well known that liquid crystals (LCs) containing chiral molecules such as the cholesteric liquid crystals (CLCs) can self-organize into an anisotropic chiral one-dimensional PC with a pitch that can be right or left handed [11]. The photonic bandgap of CLCs is polarization dependent. Circularly polarized light with a sense of rotation opposite to the LC helix is transmitted through the CLC, while for light of opposite handedness, the photon density of states vanishes in the band gap and is enhanced at the edge [12, 13]. Based on these properties, circularly polarized DFB lasers have been realized by employing CLCs to provide a permanent chiral DFB structure. Low threshold lasing was observed at the edge of the band gap in a dye doped CLC film by V.I. Vopp *et al.* [13]. Wu's group demonstrated a highly efficient laser upon band edge excitation based on dye doped CLCs [14].

In this letter, we report for the first time on dynamic circularly polarized DFB laser action. It is based on a reflection pumping configuration by polarization modulation. The medium is an isotropic DCM doped methanol solution. Dynamic chiral photonic DFB structures were obtained easily by controlling the polarization state of the two interfering beams. Tunable dual-peak circularly polarized lasing emission at the first Bragg order was achieved in left-handed circularly polarized: left-handed circularly polarized pumping (LCP:LCP pumping) and right-handed circularly polarized: right-handed circularly polarized pumping (RCP:RCP pumping) cases. The dual-peak lasing structure indicates that the chiral polarization modulation bears an index contribution in addition to the gain one. Intensity and polarization modulation dominate the feedback of the lasing oscillation at the same time. A analysis of the electric field distribution within the gain medium is presented for understanding the generation of chiral DFB structures and circularly polarized lasing output.

2. Experiments

DCM doped methanol served as the laser medium in our experiments. The dye concentration was 2×10^{-3} M. The optical arrangement shown in Fig. 1 was similar to the one used in previous work [8]. A frequency-doubled Nd:YAG laser (pulse duration = 6 ns) was employed as the pump source. A Glan-Taylor Prism was placed into the optical path to define the pump beam as *s*-polarized. This beam was divided by a 50/50 *s*-polarized beam splitter. The initial pump beam diameter was around 6 mm. This beam was focused with a 0.5 m focal length objective to increase the pump energy density. By adopting two quarter-wave plates at 532 nm, circularly polarized pumping geometries can be constructed as desired. The two pump beams of approximate equal strength were reflected onto the dye cell. They intersected inside the dye cell to create the reflection grating. A periodic modulation of gain and/or index was thus induced in the laser gain medium. The modulation period can be expressed as

$$\Lambda = \frac{\lambda_{pump}}{2n \times \sin\left(\frac{\theta_{in}}{2}\right)}, \quad (1)$$

where λ_{pump} is the pump wavelength, n is the refractive index of the gain medium at lasing wavelength λ_L , and θ_{in} is the intersection angle inside the dye cell after refraction by the solution. Combining with the Bragg condition $2n\Lambda = M \cdot \lambda_L$, where M is the Bragg reflection order, the output wavelength is obtained as an index-independent form

$$\lambda_L = \frac{\lambda_{pump}}{M \times \sin\left(\frac{\theta_{in}}{2}\right)} \quad (2)$$

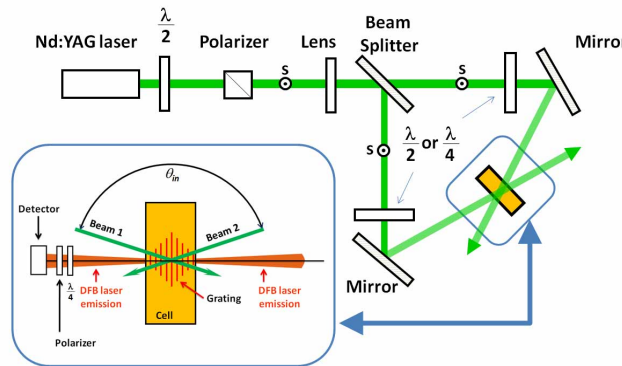


Fig. 1. Experimental set-up for reflection grating excitation. Inset shows a zoom of the cell.

The first order Bragg condition ($M=1$) was satisfied in our experiments. Tuning of λ_L was achieved by varying the intersection angle. The dye cell was slightly tilted to separate DFB from cavity lasing induced by the Fresnel reflection between dye cell edges. The lasing signal was collected by an optical fiber, then dispersed and analyzed by a 600 lines/mm grating coupled to a spectrometer in conjunction with a cooled CCD camera. The resolution limit of the detection system was 0.1 nm.

The state of polarization and the rotation angle of the DFB laser output were analyzed by a polarizer combined with a quarter-wave plate at 632.8 nm. In order to exploit the quarter-wave plate at 632.8 nm, the DFB laser output wavelength was deliberately set as around 632.8 nm, corresponding to an intersection angle inside the dye cell of 57.21 degree, which was in the range of the amplified spontaneous emission (ASE) of the DCM doped methanol solution.

Two circularly polarized pumping geometries were studied, which were LCP:LCP pumping and RCP:RCP pumping respectively. Tunable left-handed and right-handed circularly polarized DFB lasing output was thus obtained.

3. Results and discussion

3.1 LCP:LCP pumping geometry

The circularly polarized DFB laser was first operated in LCP:LCP pumping geometry. The two pumping beams were converted to have left-handed circularly polarization by properly rotating the two quarter-wave plates at 532 nm. A DFB lasing was observed when the pump energy was above 0.3 mJ after counting for reflection and transmission losses. Tuning of the output wavelength was obtained by varying the intersection angle. Dual-peak laser emission was achieved throughout the tuning range (right inset in Fig. 2). Each emission peak was split with an interval or a shoulder. The dual-peak lasing structure results from the existence of an index-type DFB grating in the gain medium, according to the coupled-wave theory of Kogelnik and Shank [15]. Detailed interpretation of the phenomenon was given in previous work [8]. The tuning behavior of the DFB laser in LCP:LCP pumping is summarized in Fig. 2. Tuning data generally follow the solid line, which is the Bragg resonance condition for the reflection configuration. The theoretical curve fits with the experimental data. The left inset in Fig. 2 shows the output intensity as a function of the pump energy near the gain center, which indicates a threshold pump energy of 0.3 mJ. Saturation of the lasing intensity under higher pump energy is also observed.

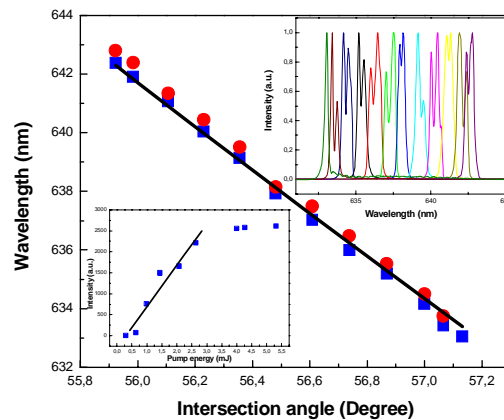


Fig. 2. Output wavelengths as a function of the internal intersection angle θ_{in} in LCP:LCP pumping geometry. The solid curve is the prediction based on the first order Bragg condition. Right inset shows the corresponding tuning spectra. The left inset shows the emission intensity versus the pump energy.

The DFB laser emission was then tuned to 632.8 nm. Using a quarter-wave plate at this wavelength and a polarizer, the polarization state and the rotation angle of the lasing output could be determined from both sides of the dye cell. The polarization state was first examined only with a polarizer. The DFB lasing intensity distribution with the azimuthal angle of the polarizer is shown in Fig. 3(a). It exhibits a roughly circular distribution in a polar plot. By inserting the quarter-wave plate at 632.8 nm between the dye cell and the polarizer, the polarization property of the DFB lasing was further examined from both the left and right side of the sample. The fast axis of the quarter-wave plate was parallel to the *s*-polarized direction. After passing through the quarter-wave plate and the polarizer, the DFB lasing intensity distribution with the azimuthal angle of the polarizer exhibits linear polarization characteristics shown in Fig. 3(b) (the left side output) and Fig. 3(c) (the right side output), respectively.

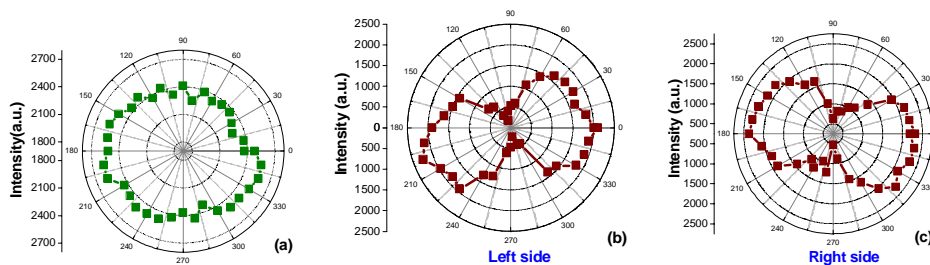


Fig. 3. Polar plots of the DFB lasing output intensity vs. the azimuthal angle of the polarizer without inserting the quarter-wave plate (a); with inserting the quarter-wave plate, measured from the left side of the dye cell (b) and the right side of the dye cell (c).

According to Fig. 3, the DFB laser emission generated in LCP:LCP pumping geometry should be circularly polarized since the polarization of the DFB lasing was successfully converted to linear polarization after transmitting through a quarter-wave plate. In addition, referring to the rotation angle of the linear polarization of the converted DFB lasing relative to the fast axis of the quarter-wave plate [Fig. 3(b) and Fig. 3(c)], the left side DFB lasing output should be identified as left-handed circularly polarized light, in contrast, the right side DFB lasing output should be a right-handed circularly polarized light.

3.2 RCP:RCP pumping geometry

The circularly polarized DFB laser was subsequently realized in RCP:RCP pumping geometry. The two interfering pump beams were converted to right-handed circular polarization. Similar results were achieved as those in LCP:LCP pumping case (shown in Fig. 4). The threshold was 0.3 mJ, the same as for LCP:LCP pumping.

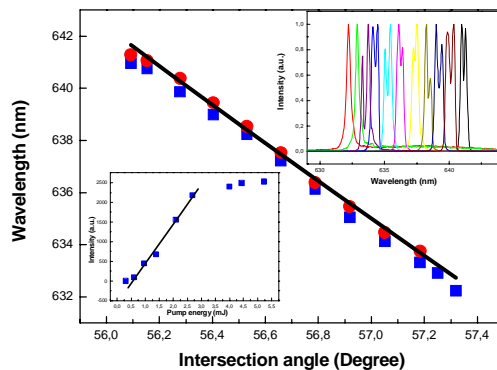


Fig. 4. Wavelength tuning as a function of the internal intersection angle θ_{in} in RCP:RCP pumping geometry. The solid curve is the theoretical fit based on the first-order Bragg condition. Right inset shows the corresponding tuning spectra. The left inset shows the emission intensity versus the pump energy.

Then the polarization property of the DFB laser emission was examined by a polarizer in combination with the quarter-wave plate at 632.8 nm. The polarization state was determined from both sides of the dye cell, similar to the LCP:LCP pumping case. Figure 5 summarizes the measurements of the DFB lasing output intensity as a function of the azimuthal angle of the polarizer. Figures 5(b) and 5(c) show lasing intensity distributions after passing through the quarter-wave plate and the polarizer for the left side and the right side laser output, respectively. As shown, the DFB laser emission in RCP:RCP pumping geometry is also

circularly polarized. In contrast to LCP:LCP pumping, the left side laser output is a right-handed circularly polarized light, while the right side laser output is a left-handed circularly polarized light.

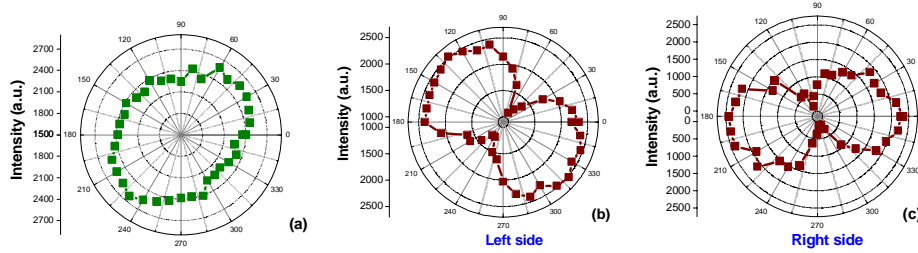


Fig. 5. Polar plots of the DFB lasing output intensity vs. the azimuthal angle of the polarizer without inserting the quarter-wave plate (a); with inserting the quarter-wave plate, measured from the left side of the dye cell (b) and the right side of the dye cell (c).

4. Analysis

The dual-peak circularly polarized DFB lasing output in our reflection DFB lasers comes from the feedback of polarization modulation, caused by a polarization grating, generated by the interference polarization field of the two pumps. In Ref. 10 and 11, it was found that, in transmission grating pumping geometry, the polarization of the DFB lasing output follows the ellipticity of the projection of the spatially varying polarization field of the interfering pump beams on the plane perpendicular to the propagation direction of the DFB laser beam. To explore the underlying physics of the polarization characteristic of our reflection DFB lasers, the interference fields on the reflection grating planes are analyzed using the electric field distribution within the gain medium. The corresponding modulation for lasing oscillation is identified by using concepts of polarization volume holograms [16, 17].

Figure 6(a) shows a simple scheme of our DFB lasers based on reflection grating geometry in the right-handed Cartesian coordinate system. The surface of the dye cell is parallel to the x-y plane in the scheme. The grating vector of the transient reflection DFB grating is perpendicular to the sample surface. When two circularly polarized pumping beams intersect inside the dye cell, the phase difference between them induces a total field, which is generally a planar ellipse, varying in magnitude and orientation in three-dimensional space with the same spatial periodicity as the corresponding intensity pattern. The interference pump fields at an arbitrary intersection angle can be written when the two exciting circular polarized beams are parallel, with left-handed rotation direction (LCP:LCP crossing) :

$$\left. \begin{aligned} \vec{E}_1 &= \frac{1}{\sqrt{2}} \left[\hat{x}iE + \hat{y}E \sin\left(\frac{\theta_{in}}{2}\right) + \hat{z}E \cos\left(\frac{\theta_{in}}{2}\right) \right] e^{-ik_1 \cdot r} \\ \vec{E}_2 &= \frac{1}{\sqrt{2}} \left[\hat{x}iE - \hat{y}E \sin\left(\frac{\theta_{in}}{2}\right) + \hat{z}E \cos\left(\frac{\theta_{in}}{2}\right) \right] e^{-ik_2 \cdot r} \end{aligned} \right\} \quad (3)$$

$$\Rightarrow \vec{E}_{LCP:LCP} = \frac{1}{\sqrt{2}} E \left[\hat{x}i(1 + e^{-i\varphi}) + \hat{y}(e^{-i\varphi} - 1) \sin\left(\frac{\theta_{in}}{2}\right) + \hat{z}(e^{-i\varphi} + 1) \cos\left(\frac{\theta_{in}}{2}\right) \right]$$

Where k_1 and k_2 are the wave vectors, r is the position vector, $\varphi = (k_1 - k_2) \cdot r$ is the phase difference between the two pumping beams; assuming that the amplitudes E for the two beams are same; θ_{in} is the intersection angle. \hat{x} , \hat{y} and \hat{z} are unit vectors. When the two exciting circular polarized beams are parallel, with right-handed rotation direction (RCP:RCP crossing), the interference pump fields can be written as :

$$\begin{aligned}
 \vec{E}_1 &= \frac{1}{\sqrt{2}} \left[-\hat{x}iE + \hat{y}E \sin\left(\frac{\theta_{in}}{2}\right) + \hat{z}E \cos\left(\frac{\theta_{in}}{2}\right) \right] e^{-ik_1 r} \\
 \vec{E}_2 &= \frac{1}{\sqrt{2}} \left[-\hat{x}iE - \hat{y}E \sin\left(\frac{\theta_{in}}{2}\right) + \hat{z}E \cos\left(\frac{\theta_{in}}{2}\right) \right] e^{-ik_2 r} \\
 \Rightarrow \vec{E}_{RCP:RCP} &= \frac{1}{\sqrt{2}} E \left[-\hat{x}i(1 + e^{-i\varphi}) + \hat{y}(e^{-i\varphi} - 1) \sin\left(\frac{\theta_{in}}{2}\right) + \hat{z}(e^{-i\varphi} + 1) \cos\left(\frac{\theta_{in}}{2}\right) \right]
 \end{aligned} \quad (4)$$

From Eqs. (3) and (4), pictorial representations of the interference patterns on the plane perpendicular to the propagation direction of the laser beam (x-y plane) can be deduced.

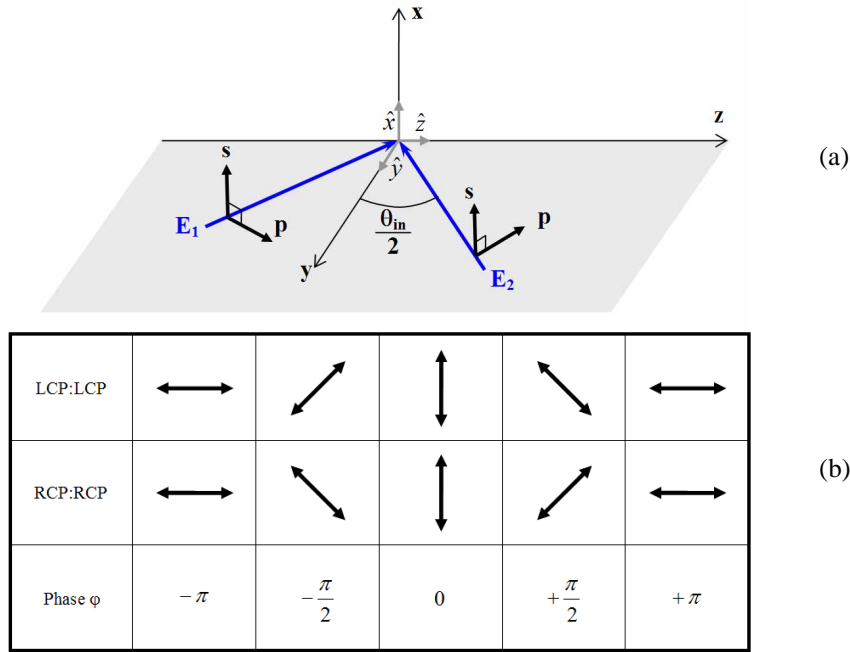


Fig. 6. (a). Scheme of the reflection pumping geometry in the right-handed Cartesian coordinate system; (b). One period of the polarized interference field pattern is projected onto the x-y plane for the two types of reflection pumping schemes (the upper row is for LCP:LCP pumping and the lower one for RCP:RCP pumping).

In Fig. 6(b), one period of the polarized interference field patterns projected onto the x-y plane at the intersection angle of 57.21 degree, for LCP:LCP and RCP:RCP pumping geometries is illustrated, respectively. In LCP:LCP pumping, the interference pattern on the x-y plane presents left-handed helical structure, while a right-handed helical structure is obtained in RCP:RCP pumping. The intensity of the total incident fields is spatially varying according to Eqs. (3) and (4). The polarization states are everywhere linear but rotate in space with a constant angular frequency along the grating period. The reflection gratings are not only intensity gratings but also polarization gratings. Thus the modulations are a combination of both intensity and polarization modulation. The excited dipoles of the dye molecules have a rotating distribution along the x-y plane; this determines that the DFB lasing output will be a circularly polarized beam. The difference between LCP:LCP and RCP:RCP pumping cases is that the rotation sense of the interference field is opposite; this determines the rotation direction of the circularly polarized DFB lasing.

Referring to the laser action in chiral photonic structures composed of dye doped CLCs [11], in our reflection DFB lasers, left-handed and right-handed chiral photonic structures are created in LCP:LCP pumping and RCP:RCP pumping, respectively. Left-handed and right-handed circularly polarized lasing output are respectively obtained from the left and right side of the sample in LCP:LCP pumping geometry. The reverse situation is achieved in RCP:RCP pumping geometry. In lasing chiral structures, the circular polarization is usually the same on both sides of the sample. As a possible explanation for the difference with our present results, there might be retardation between the two pump beams within the dye cell, so that the handedness of the grating created changes with depth into the sample. Such retardation may be caused by the non uniformity of the pump intensities with the cell, following absorption by the dye. So, a simple means to realize chiral photonic structures was demonstrated based on our DFB lasers in reflection pumping configuration, by manipulating the polarization state of two pumping beams, meanwhile, the polarization modulation was also proven effective in feedback for the DFB lasing action. The induced chiral DFB photonic structures can also be identified as a chiral PC [11] with tunable PBG, which was evidenced by the tunable spectral intervals of the dual- lasing emission peaks; the PBG was polarization dependent, which was demonstrated by the polarization property of the lasing output. Additionally, splitting of the circularly polarized laser emission shows that the index-type polarization grating is not a thermal effect due to heating by the pump but the resonant nonlinearity of the DCM dye [8].

5. Conclusion

In this work, we realized tunable circularly polarized DFB laser emission based on reflection grating configuration in DCM doped methanol. Transient chiral photonic DFB structures were induced by crossing two circularly polarized pumping beams of the same handedness. Both intensity modulation and polarization modulation dominated the lasing feedback. A light-induced index-grating caused by intensity modulation contributed to the generation of the dual-peak lasing emission, while the polarization modulation effectively controlled the polarization property of the laser output. Tunable circularly polarized lasing emission for the first Bragg order was observed in both LCP:LCP and RCP:RCP pumping geometries. The rotation angle of the circularly polarized lasing output was diagnosed by analyzing the total pumping electric field distribution within the gain medium. The tunability and threshold of the DFB laser emission were also studied. We have demonstrated reflection DFB lasers by polarization modulation as a new method to realize transient chiral photonic structures and to achieve circularly polarized lasing output.

Acknowledgments

Research at Queen's University is supported by the Natural Sciences and Engineering Research Council and the Canada Research Chair program on Chiral Photonics.

Tunable circularly polarized lasing emission in distributed feedback dye lasers

Chen, Fei

2008-10-13T00:00:00Z

This paper was published in Optics Express and is made available as an electronic reprint with the permission of OSA. The paper can be found at the following URL on the OSA website: <http://www.opticsinfobase.org/oe/abstract.cfm?uri=oe-16-21-16746> Systematic or multiple reproduction or distribution to multiple locations via electronic or other means is prohibited and is subject to penalties under law.

Fei Chen, Denis Gindre, and Jean-Michel Nunzi, Tunable circularly polarized lasing emission in distributed feedback dye lasers, Optics Express, 2008, Volume 16, Issue 21, Pages 16746-16753.

<http://dx.doi.org/10.1364/OE.16.016746>

Downloaded from CERES Research Repository, Cranfield University